Magnetotunneling from accumulation layers in $Al_xGa_{1-x}As$ capacitors

T. W. Hickmott
IBM Thomas J. Watson Research Center, Yorktown Heights, New York 10598
(Received 26 June 1985)

Current-voltage (I-V), ac capacitance-voltage (C-V), and conductance-voltage (G-V) measurements have been made of the effect of magnetic fields up to 15 T on tunneling at 1.6 K from accumulation layers on n-type GaAs. The samples used are n^--GaAs—$Al_xGa_{1-x}As$—n^+-GaAs capacitors in which the GaAs/$Al_xGa_{1-x}As$ barrier height is low enough, ~0.3 eV, and the $Al_xGa_{1-x}As$ is thin enough, ~20 nm, that direct tunneling of electrons occurs. Magnetic freezeout of carriers in n^--GaAs for $H \gtrsim 4$ T can be determined from C-V curves. For n^+-GaAs biased positive, $V_G > 0$, a quantized accumulation layer forms at the n^--GaAs/$Al_xGa_{1-x}As$ interface. Structure is observed in I-V, C-V, and G-V curves due to tunneling from Landau levels in the accumulation layer. Two samples are compared in detail. In one sample the Landau-level structure is relatively simple. In the other, spin splitting is observed in the first three Landau levels. The dependence of the surface concentration of electrons on V_G is determined from tunneling currents at fixed V_G and varying magnetic field. A second subband in the accumulation layer begins to be populated when the surface concentration $\gtrsim 7\times10^{11}/cm^2$. This is the first example of a system in which it is possible to use tunneling to examine the formation of an accumulation layer in a semiconductor, going from depletion through flat-band into accumulation, by applying a bias voltage.

INTRODUCTION

The potential well that forms when a high electric field is applied to a semiconductor surface quantizes electron motion perpendicular to the surface.[1] Although quantization of electron motion occurs in either accumulation or inversion layers on semiconductors, accumulation layers have been studied much less than inversion layers. Ben-Daniel and Duke[2] initially proposed that tunneling could provide information about accumulation layers. Tsui, in a series of papers,[3–9] used tunneling to study accumulation layers on InAs. He used InAs-oxide-Pb structures in which a thin-oxide layer was grown thermally on degenerate InAs single crystals. The accumulation layer formed during oxidation, presumably due to positive charge in the oxide layer, though the detailed mechanism for its formation was not clear. Appelbaum and Baraff[10,11] discussed the theory of tunneling in such structures. Other semiconductors for which tunneling has been used to study accumulation layers include PbTe,[12] ZnO,[13] Si,[14,15] InSe,[16] Te,[17,18] and HgCdTe.[19] In every case the accumulation layer was formed during sample preparation and the properties were fixed. In no case has it been possible to study the formation of an accumulation layer, starting from depletion, by changing the electric field at the semiconductor surface. Recently we have shown that undoped $Al_xGa_{1-x}As$ is a nearly ideal dielectric in n^--GaAs—undoped $Al_xGa_{1-x}As$—n^+-GaAs capacitors.[20,21] Capacitance-voltage (C-V) characteristics of $Al_xGa_{1-x}As$ capacitors are nearly ideal; they can be modeled by classical semiconductor-insulator-semiconductor (SIS) theory, assuming that there are no interface states at the insulator-semiconductor interface. Current-voltage (I-V) characteristics of $Al_xGa_{1-x}As$ capacitors at low voltages, between 100 and 300 K, are dominated by thermionic emission. Barrier heights at the GaAs/$Al_xGa_{1-x}As$ interface can be determined by analysis of the temperature dependence of I-V characteristics. The principal nonideality of undoped $Al_xGa_{1-x}As$ as a capacitor dielectric is the occurrence of a uniform density of negative charge. Band bending due to negative charge in $Al_xGa_{1-x}As$ increases barrier heights at the n-GaAs/$Al_xGa_{1-x}As$ interfaces, measured by analysis of I-V curves, and shifts C-V curves to voltages more positive than expected from simple SIS theory. If V_G is the voltage applied to the n^+-type GaAs gate, the flat-band voltage V_{FB} of an AlGaAs capacitor having no negative space charge should occur when V_G is slightly negative. Negative charge densities can be large enough that positive values of V_{FB} are observed. The amount of negative charge depends in an unknown way on sample-preparation conditions.

At low temperatures and high fields, tunneling is the principal conduction mechanism in thick-AlGaAs capacitors. Resonant Fowler-Nordheim tunneling is observed in $Al_xGa_{1-x}As$ capacitors that are between 30 and 40 nm thick.[22] The low barrier height at the $Al_{0.4}Ga_{0.6}As$/GaAs interface (~0.3 eV) and the low effective mass in $Al_xGa_{1-x}As$ (~$0.1m_0$, where m_0 is the free-electron mass) means that direct tunneling is observed in $Al_xGa_{1-x}As$ capacitors that are about 20 nm thick.

Electrons in an accumulation or inversion layer can move freely, parallel to the semiconductor interface. Application of a magnetic field perpendicular to the surface quantizes carrier motion parallel to the surface and splits the constant density of states of a two-dimensional electron gas (2DEG) into Landau levels. Structure in tunneling curves due to Landau levels has been observed in tunnel diodes and in tunneling from accumulation layers on InAs.[3,4,23,24] Structure in C-V curves due to carriers in

 ©1985 The American Physical Society

Landau levels in inversion layers provided early evidence for quantization in 2DEG's.[25] C-V curves have recently been used to derive a density of states in Landau levels in the 2DEG of modulation-doped heterostructures.[26] C-V curves in these cases are for electron motion parallel to the semiconductor-insulator interface.

Here we report observations of the effect of magnetic fields between 0 and 15 T on ac capacitance-voltage and conductance-voltage (G-V), and on dc I-V curves of Al-GaAs capacitors. Several different phenomena are observed. For magnetic fields greater than ~ 4 T, magnetic freezeout occurs in n^--type GaAs. The high-series resistance produced by magnetic freezeout distorts C-V curves at high frequencies. When the n^+-type GaAs gate of an AlGaAs capacitor is biased positively, an accumulation layer forms on n^--type GaAs. Tunneling currents in high magnetic fields show structure due to Landau levels in the accumulation layer. From their dependence on magnetic field we obtain the dependence of surface electron concentration N_S on gate voltage and show that population of a second subband begins when N_S exceeds $\sim 7\times 10^{11}/\text{cm}^2$. When the n^+ gate is biased negatively, electrons tunnel from n^+-type GaAs into n^--type GaAs. We attribute structure with a period of 0.036 V observed in I-V curves of some samples to sequential single-phonon emission in n^--type GaAs due to ballistic electrons in frozen-out GaAs.[27,28] The $Al_xGa_{1-x}As$ capacitor is the first system in which one can move the Fermi level in a semiconductor by applying voltage so that it is possible to go from depletion through flat band into accumulation and use tunneling to determine properties of the accumulation layer. It is close to an ideal structure to study tunneling: substrate, insulator, and gate are all single crystals with closely matched lattice spacing in all three layers.

THEORETICAL BACKGROUND

The n^--GaAs—undoped $Al_{0.4}Ga_{0.6}As$—n^+-GaAs capacitors used in this work are shown schematically in the potential-energy diagrams of Fig. 1. The capacitor is shown with $V_G > V_{FB}$ in Fig. 1(a) so that the n^--type GaAs is biased into accumulation. V_G is the voltage applied to the n^+-type GaAs gate. The applied voltage divides into three terms: ψ_S, the band bending in the substrate; ψ_G, the band bending in the gate; and V_I, the voltage drop across the insulator. For $V_G > V_{FB}$, $V_I > \psi_S \gtrsim \psi_G$. Electrons in the accumulation layer are quantized in the direction perpendicular to the interface. Two subbands, E_0 and E_1, are indicated in the accumulation layer; E_F is between them so only E_0 would be occupied at low temperature. We take the n^--type GaAs to be nondegenerate in Fig. 1(a) since this corresponds to the experimental situation in the present work. This is in contrast with Tsui's measurements of tunneling from degenerate InAs or PbTe, in which tunnel currents were due to bulk electrons as well as to electrons in an accumulation layer. In Fig. 1(b), $V_G < V_{FB}$ and a depletion layer forms in the n^--type GaAs substrate. The largest fraction of V_G is used to form the depletion region; $\psi_S > V_I > \psi_G$, since there is little change in ψ_G with bias for $V_G < V_{FB}$. No accumulation layer forms on the n^+-type GaAs because of its high doping.

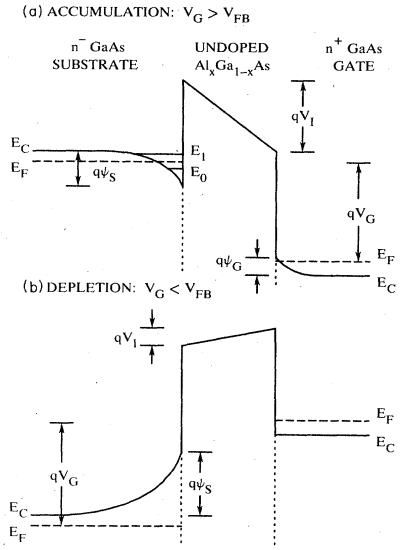

FIG. 1. (a) Schematic energy-band diagram for n^--GaAs—undoped $Al_xGa_{1-x}As$—n^+-GaAs capacitor in accumulation showing two subbands. (b) Schematic energy-band diagram of capacitor in depletion.

For zero magnetic field the density of states in each of the subbands of the accumulation layer is constant in energy as indicated schematically in Fig. 2(a). If E_i is the minimum energy of subband i, $E_i - E_C$ and $E_F - E_C$ depend on surface field and therefore increase as V_G increases. When a magnetic field H is applied perpendicular to the GaAs/$Al_xGa_{1-x}As$ interface it quantizes each two-dimensional subband into discrete Landau levels, as indicated schematically for the lowest subband, E_0, in Fig. 2(b). If there were no level broadening, the density of states would be a series of δ functions. The energy of the Landau levels for the lowest subband is given by

$$E = E_0 + \left[N + \frac{1}{2}\right]\frac{e\hbar H_z}{m} \pm \frac{g\mu_B H}{2}, \quad N = 0,1,2,\ldots \tag{1}$$

where N is the Landau-level index, H_z is the component of magnetic field perpendicular to the surface, e is the electron charge, m is the effective mass of electrons, μ_B is the free-electron Bohr magneton, and g is the g factor of the electron. For an effective mass for GaAs of $0.067m_0$, where m_0 is the free-electron mass, the cyclotron energy becomes

$$\hbar\omega_c = \frac{eH_z\hbar}{m} = 1.73H_z\,(\text{T})\ \text{meV}\ . \tag{2}$$

Equation (1) ignores the effect of the magnetic field on the spread of the wave function in the accumulation layer.[1,5] The number of carriers per Landau level is

$$N_L = \frac{eH_z}{h} = 4.836\times 10^{10} H_z\,(\text{T})\ \text{cm}^{-2} \tag{3}$$

if spin splitting is not resolved, as in Fig. 2(b). In practice, Landau levels are broadened as indicated schemati-

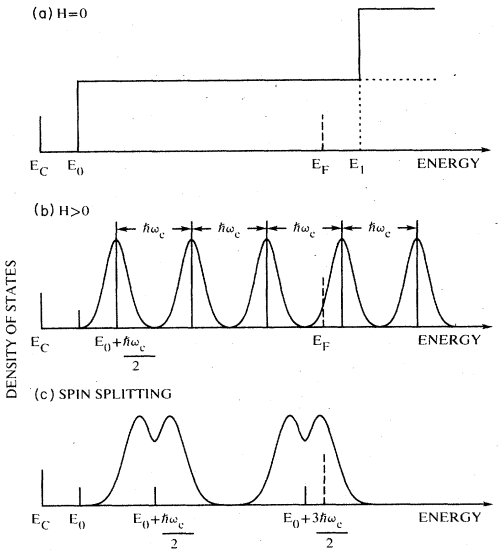

FIG. 2. (a) Schematic density of states in a two-dimensional electron gas when magnetic field is zero. (b) Effect of magnetic field on density of states in a two-dimensional electron gas. (c) Schematic diagram of spin splitting of Landau levels in a two-dimensional electron gas.

cally by the Gaussian line shapes in Fig. 2(b). The radius of the lowest cyclotron orbit of an electron in a magnetic field is $l=(\hbar/eH)^{1/2}=25.66[H\,(\mathrm{T})]^{-1/2}$ nm. When a magnetic field is applied parallel to the AlGaAs/GaAs interface, Landau levels are no longer observed in an accumulation layer although spin-splitting remains unchanged.

Figure 2(c) shows schematically the case of the Landau level split due to spin interactions. The density of states at the center of a Landau level is no longer a maximum but becomes a local minimum. In Figs. 2(b) and 2(c) increasing V_G increases N_S, the concentration of electrons per cm^2 in the accumulation layer, and therefore increases $E_F-(E_0+\hbar\omega_c/2)$. At constant H, after the threshold voltage V_T for establishing an accumulation layer is exceeded, the Fermi level moves through successive maxima and minima in the density of states. If V_G is held constant, increasing H moves successive maxima and minima in the density of states through E_F. V_G determines the number density of carriers in the accumulation layer; it is not simply related to E_F-E_i. Complicating any correlation of V_G and E_F is the requirement that the Fermi level jump abruptly from one Landau level to the next as each level either empties or completely fills.[29]

EXPERIMENTAL

The sample preparation and processing to form AlGaAs capacitors has been described previously.[21,30] The samples were grown on ⟨100⟩-oriented single-crystal n^+-type GaAs substrates. We give detailed results on two samples, sample A (1019A4,6 in Ref. 21) and sample B (1332D4 in Ref. 21). The AlAs mole fraction is 0.4 for sample A and 0.37 for sample B. Sample characteristics including insulator thickness w, barrier heights at the n^+-GaAs/$Al_{0.4}Ga_{0.6}As$ interface, ϕ_G, and negative charge in $Al_{0.4}Ga_{0.6}As$ were measured for each sample and are shown in Table I. N_M is the substrate doping, N_G is the gate doping, and N_I is the amount of negative charge in the undoped $Al_xGa_{1-x}As$ layer, determined from the shift of experimental C-V curves to positive voltages with respect to their calculated flat-band voltages. N_M, N_G, and w were determined by modeling C-V curves, assuming a dielectric constant of $Al_{0.4}Ga_{0.6}As$ of 11.8 at 300 K. The tunneling thickness is about 3 nm smaller than w.[22] The sample designations A and B are the same as in Ref. 21. The samples were mounted on nonmagnetic eight-pin TO-5 headers with conducting epoxy. Sample areas were 4.13×10^{-4} cm^2.

C-V curves between 1 kHz and 1 MHz were measured with an HP 4274A or 4275A multifrequency LCR meter. The LCR meter measures the impedance of the $Al_xGa_{1-x}As$ capacitor as a parallel capacitance, $C(V)$, and conductance, $G(V)$. Four-probe measurements are used for best accuracy. To avoid distortions of C-V curves the ac voltage that is superimposed on the dc-bias voltage should be less than k_BT. This is not possible at 1.6 K, where $k_BT\sim0.14$ meV. Instead, ac voltages of ~5 mV rms were used. The dc—I-V curves were measured with a two-channel auto-ranging Keithley 619 electrometer. The useful current range of the meter is from $\sim5\times10^{-12}$ to 2×10^{-2} A. V_G was varied in 5-mV increments. All electrical measurements were controlled by an IBM Series/1 computer. Magnetic field measurements were made in a superconducting magnet with the sample immersed in pumped helium at 1.6 K.

RESULTS

For both samples studied, magnetic freezeout of n^--type GaAs produces a high-series resistance that seriously affects C-V measurements at high frequencies and high magnetic fields. Both samples show the effect of Landau levels on tunneling from an accumulation layer. For sample A, the Landau-level structure is relatively simple in the C-V, G-V, and I-V curves. For sample B, spin-splitting of Landau levels produces complex structure in tunneling curves which is resolved in both dc and ac characteristics. dc and ac measurements complement each other in studying the formation of an accumulation layer on n^--type GaAs. Recently, we have reported the occurrence of periodicities in I-V characteristics when electrons tunnel into n^--type GaAs.[27,28] The periodicities were attributed to sequential single-phonon emission by electrons tunneling from n^+-type GaAs into n^--type GaAs. As reported, sample A shows such effects very clearly. Sample B does not show periodicities whose magnitude increases with magnetic field.

Sample A

Magnetic freezeout

Analysis of C-V curves of $Al_xGa_{1-x}As$ capacitors at 77 K and above shows that undoped $Al_xGa_{1-x}As$ may contain negative charge uniformly distributed throughout the insulator.[21] The effect of negative charge is to shift the flat-band voltage of C-V curves by an amount ΔV_{SH}

TABLE I. Properties of $Al_xGa_{1-x}As$ capacitors.

Sample	Number (in Ref. 21)	N_M (10^{15} cm^{-3})	N_G (10^{18} cm^{-3})	w (nm)	N_I (10^{16}cm^{-3})	ΔV_{SH} (V)	ϕ_G (V)	C_I at 1.6 K (pF)
A	1019A4,6	1.4	1.9	20.7	8.0	0.087	0.327	186
B	1332D4	2.1	0.9	22.0	3.6	0.029	0.296	176

to voltages more positive than expected from the difference in Fermi levels of substrate and gate, to bend the conduction band in the $Al_xGa_{1-x}As$, and to increase the barrier height for thermionic emission at both $GaAs/Al_xGa_{1-x}As$ interfaces. From analysis of experimental C-V curves by a classical SIS model that ignores quantum effects in the accumulation layer, we obtain ΔV_{SH}, the insulator capacitance C_I, and the difference of Fermi levels for gate and substrate, measured with respect to the conduction-band edge, $\eta_G-\eta_S$. We also obtain V_{FB} for experimental curves, the value of V_G at which there is no band bending in n^--type GaAs. These quantities are shown as a function of temperature for sample A in Fig. 3. ΔV_{SH} is constant between 77 and 250 K. If there were no negative charge $\eta_G-\eta_S$ would equal V_{FB} and both would be negative. Due to negative charge, V_{FB} is less negative than $\eta_G-\eta_S$. Because of the neglect of quantum effects, the SIS model becomes progressively less accurate below 77 K; we estimate the values of C_I and V_{FB} at 1.6 K by extrapolating the higher-temperature data. $V_{FB}\sim 0.052$ V at 0 K. C_I also depends linearly on temperature below 150 K because of the temperature dependence of the insulator dielectric constant ϵ_I. The value of C_I at 1.6 K is obtained by extrapolation and is given in Table I.

Magnetic freezeout of electrons onto donors in semiconductors can occur in high magnetic fields when the dimensionless parameter $\gamma=\hbar\omega_c/(2R)\sim 1$, where R is the Rydberg energy of the shallow donor and $\hbar\omega_c$ is the cyclotron energy of a conduction-band electron in the magnetic field.[31] For GaAs this condition is met at $H\sim 6.4$ T. When $H=6.4$ T the radius of the cyclotron orbit of a conduction-band electron, l, is approximately equal to the Bohr radius of the donor in GaAs, 10 nm. C-V curves at low temperature and high magnetic field show that magnetic freezeout of carriers occurs in n^--type GaAs. C-V and $\log_{10}G$-V (G-V) curves at 100 kHz, and at different magnetic fields are shown in Fig. 4. Neither the C-V nor the G-V curve at 0 T has structure. At 4 T for $V_G>0$ V, there is structure in both curves due to Landau levels in the accumulation layer that forms on the n^--type GaAs.[32] At higher magnetic fields the structure due to each Landau level shifts to progressively higher voltages. For all curves, the maximum V_G is limited by the magnitude of ac conductance due to tunneling from the accumulation layer.

Evidence for magnetic freezeout in n^--type GaAs comes from the behavior of C-V curves for $V_G<0$ V, where a depletion layer forms in n^--type GaAs. As H increases, capacitance for negative V_G becomes progressively lower, C-V curves become flatter, and the steep rise in capacitance after the accumulation layer forms shifts to higher voltages and is displaced from the conductance rise. Figure 5(a) shows the depletion region of the C-V curves at different magnetic fields on an enlarged scale. At 0 and 2 T, C-V curves are nearly identical. At 4 and 6 T there is a pronounced decrease in capacitance, but there is still curvature of the C-V curves in depletion. Above 8

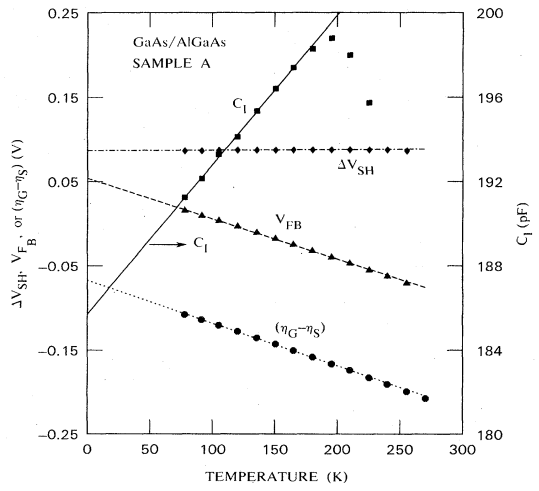

FIG. 3. Plots of best-fit parameters for calculated and measured capacitance-voltage curves of $Al_{0.4}Ga_{0.6}As$ capacitor at different temperatures.

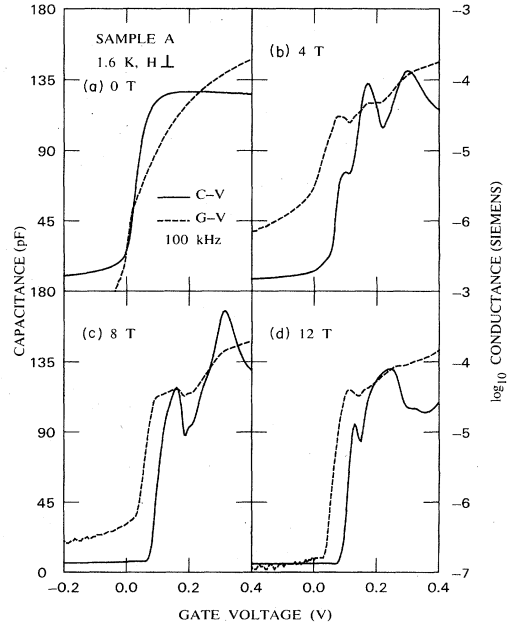

FIG. 4. Capacitance-voltage and $\log_{10}$ conductance-voltage curves at 100 kHz and at different magnetic fields for sample A.

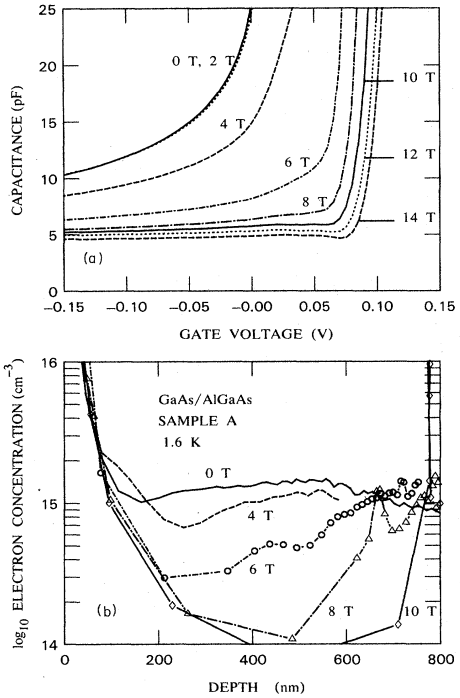

FIG. 5. (a) Capacitance-voltage curves at 100 kHz in depletion for different values of magnetic field for sample *A*. (b) Carrier-concentration profiles for different magnetic fields derived from capacitance-voltage curves.

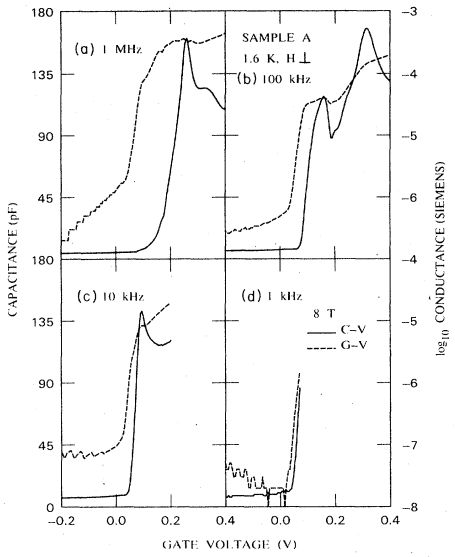

FIG. 6. Capacitance-voltage and $\log_{10}$ conductance-voltage curves at different frequencies and at a constant magnetic field of 8 T for sample A.

T the *C-V* curve for $V_G < 0$ V is nearly flat and the total capacitance corresponds to that expected for a capacitor with an insulator thickness of 1 μm and a dielectric constant corresponding to that of GaAs. The total thickness of n^--type GaAs is ≈ 1 μm.

Carrier concentration versus distance from the n^--GaAs/$Al_xGa_{1-x}As$ interface can be determined from *C-V* curves of AlGaAs capacitors in depletion by using standard metal-oxide-semiconductor (MOS) methods.[33] Such electron-concentration profiles are given in Fig. 5(b). At 0 and 2 T the average carrier concentration is 1.4×10^{15}/cm^3 which is the same as at 77 K or higher. At 4 T the average carrier concentration decreases to 1×10^{15}/cm^3. At 6 T the average concentration is $\sim5\times10^{14}$/cm^3. At higher fields the apparent carrier concentration drops further, but accuracy of the numerical values of carrier concentration is uncertain since only capacitances for voltages greater than the dip in capacitance at 0.070—0.080 V are used in determining carrier profiles.

The series resistance due to magnetic freezeout of n^--type GaAs markedly affects the frequency dependence of *C-V* curves, as shown in Fig. 6. *C-V* and *G-V* curves at a constant value of *H*, 8 T, and at different frequencies are shown. The rise in conductance at $\sim$0.030 V is independent of frequency. At 1 kHz the steep rises in *C* and *G* nearly coincide; the *C-V* curves are shifted to higher voltages at higher frequencies. The maximum voltage at which the *LCR* meter measures the sample impedance depends primarily on the magnitude of conductance. One can determine *C* and *G* at higher voltages at higher frequencies, but *C-V* curves are shifted and distorted by series resistance. The shape of *G-V* curves is less distorted at high frequencies and the structure is better resolved than for *C-V* curves. Most *C-V* curves reported here are at 100 kHz, since detailed structure in conductance is preserved and it is possible to go to higher positive values of V_G than at lower frequencies.

When going from depletion to accumulation one passes through the flat-band voltage where the carrier concentration in n^--type GaAs is constant up to the GaAs/$Al_xGa_{1-x}As$ interface. This is also the threshold voltage for the formation of an accumulation layer, V_T. *C-V* curves are too much affected by series resistance to use in determining V_T. However, the voltage at which $\log_{10}G$ rises abruptly in Fig. 6, 0.030 V, is independent of frequency and agrees well with the value of V_T that is derived later by using tunneling curves to determine the surface carrier concentration.

C-V curves calculated by classical SIS theory can be used to determine how V_G divides into its component terms ψ_S, ψ_G, and V_I as indicated schematically in Fig. 1. In Fig. 7 the different terms contributing to V_G are plotted for sample *A* at 1.6 K. In forward bias, the principal voltage drop is across the insulator; however, band bending in the gate and the substrate are approximately equal and are a significant fraction of the total applied voltage. In reverse bias, nearly all the applied voltage goes to form the depletion layer. As shown in the inset of Fig. 7, as N_M is reduced from 10^{15} to 10^{13}, V_I for $V_G = -1.0$ V decreases from 50 to 4 mV. From such model calculations, a reduction in carrier concentration in n^--type GaAs due to magnetic freezeout implies that nearly all V_G is applied across n^--type GaAs at high values of *H* for $V_G < V_{FB}$.

For $V_G = -1.0$ V, the field across 1 μm of n^--type GaAs is $\sim10^4$ V/cm. For bulk GaAs, fields of 10—20 V/cm are sufficient to ionize neutral donors and cause

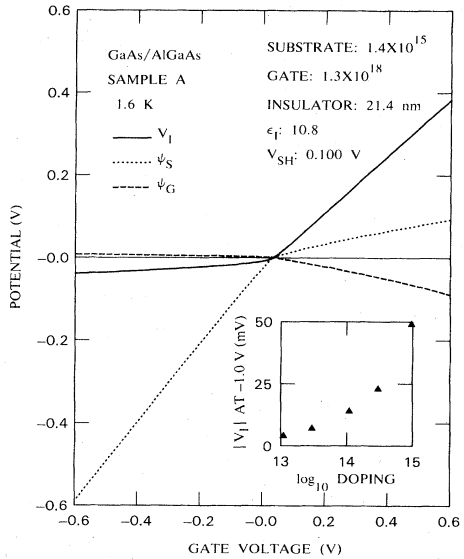

FIG. 7. The dependence of calculated values of parameters ψ_S, ψ_G, and V_I that contribute to V_G on V_G. The parameters of the calculation approximate those of sample A. The inset shows the dependence of V_I at -1.0 V for varying values of substrate doping.

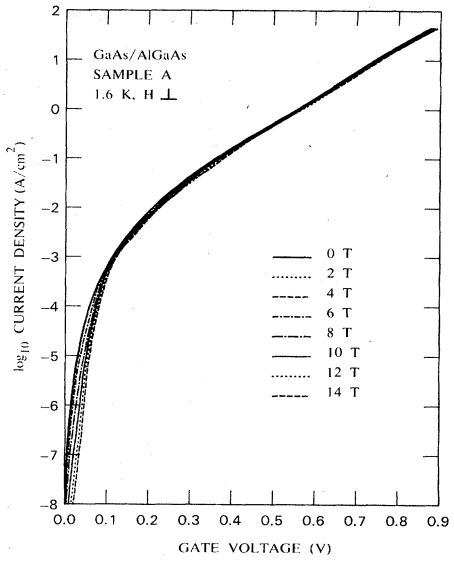

FIG. 8. $\log_{10}$ current density versus gate voltage for sample A at different magnetic fields.

avalanche multiplication due to impact ionization of carriers, even in the presence of high magnetic fields.[34] We see no evidence for such ionization processes since, for $B \gtrsim 8$ T, the capacitance is nearly constant for both positive and negative electric fields around V_T as well as for V_G up to -1.0 V. Ionization of neutralized donors, if it occurred, would leave behind positively charged donors. From Poisson's equation such donors would produce curvature of C-V curve as in the 0—6 T C-V curves of Fig. 4. Such curvature is not observed. Three factors may assist in sustaining magnetic freezeout of n^--type GaAs, even in the presence of high electric fields. One is the increased donor binding energy in high magnetic fields. Poehler's[34] Hall-effect measurements show that the donor binding energy for GaAs samples with $N_M \sim 1\times10^{15}/\text{cm}^3$ increases from 1.5 to 6 meV between 0 and 5 T. If his results can be extrapolated linearly, they would give a donor binding energy of ~ 15 meV at 14 T. Both the probability of an electron tunneling from a donor to the conduction band and the impact ionization coefficient decrease strongly as donor binding energy increases. A second factor may be limitation of the total current by the $Al_xGa_{1-x}As$ tunnel barrier. In contrast to bulk samples, current in AlGaAs capacitors is strictly limited by the barrier, making carrier multiplication and avalanching less likely than in bulk GaAs. The third factor is the possibility that the mean free path of electrons in n^--type GaAs is comparable to the thickness of the substrate[35] so that avalanche multiplication does not occur.

Tunneling from accumulation layers

Figure 8 shows the effect of H on I-V characteristics of sample A for $V_G > 0$ V. For the sample at 1.6 K $V_{FB} = V_T \cong 0.030$ V. When $V_G = 0$ V there is a small amount of band bending and a depletion layer in the GaAs substrate due to negative charge in the $Al_xGa_{1-x}As$ layer. When V_G is increased, n^--type GaAs goes through flat band and then an accumulation forms. Applying a magnetic field splits each of the subbands of the accumulation layer into Landau levels as shown schematically in Fig. 2(b). In Fig. 8 there is a substantial decrease in current for $0 < V_G \lesssim 0.1$ V as H increases. For $V_G > 0.1$ V the effect of H is not large; there is relatively little difference in I-V curves taken in dif-

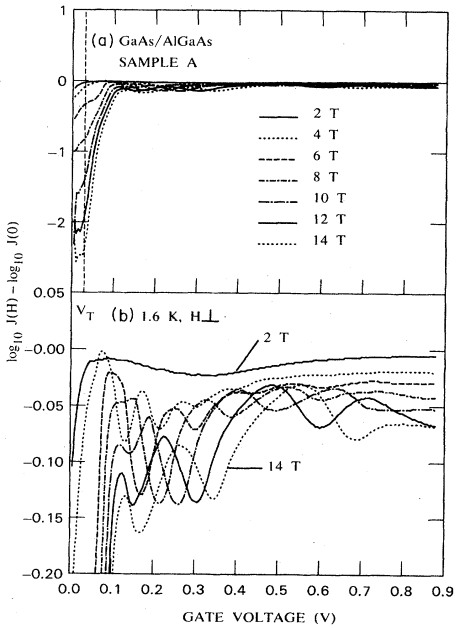

FIG. 9. Difference between $\log_{10}J$ at magnetic field H and $\log_{10}J$ at zero magnetic field as a function of gate voltage for sample A.

ferent magnetic fields. The effect of Landau levels in the accumulation layer on tunneling is shown clearly in Fig. 9, in which the difference of current densities in magnetic field H, $J(H)$, and at zero magnetic field $J(0)$, is plotted as a function of V_G for different values of H. In Fig. 9(a) the log scale is large, emphasizing the large effect of H on J when $V_G < V_T$. The current is smaller by more than two decades at 14 T than 0 T for $V_G < V_T$. The dashed-vertical line is drawn at $V_T = 0.030$ V, where inflections in the difference curves coincide closely with V_T and the curves rise abruptly above V_T. In Fig. 9(b) an expanded scale is shown and periodicities whose spacing is proportional to H are clearly seen. Structure is not well resolved for 2 T. For 4 T periodicities are resolved for $V_G < 0.4$ V and their spacing increases at higher magnetic fields. At 8 T the first maximum shows slight splitting at $V_G = 0.13$ V; the splitting is resolved at higher magnetic fields.

The fan diagram for sample A is shown in Fig. 10. Values of V_G at which extrema occur are plotted for each value of magnetic field. The lines are least-squares fits of the points at low V_G. The minima, connected by solid lines, give the best-defined linear plots; they represent the completion of the occupation of Landau levels and the beginning of the occupation of a higher level. Their common intercept is ~ 0.040 V, in reasonable agreement with threshold voltage of 0.030 V from G-V curves or the extrapolated value of 0.050 V from Fig. 3. The first maximum at ~ 0.1 V, which represents the completion of the establishment of the accumulation layer, does not shift with magnetic field to the extent that other extrema do. The splitting of the maxima of the first Landau level is proportional to H. Values of the Landau-level indices, N, are given.

When H is constant and V_G varies as in Figs. 8–10, the sequence of Landau levels for each subband is fixed by H and the Fermi level sweeps through the Landau levels.

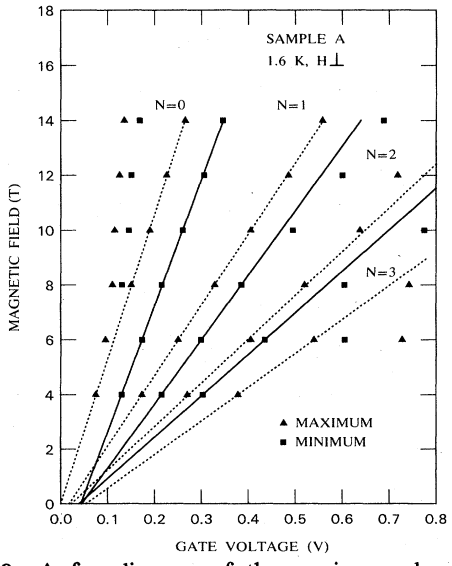

FIG. 10. A fan diagram of the maxima and minima of $\log_{10}J(H)$-$\log_{10}J(0)$ for sample A. The solid lines are least-squares fits of minima, the dotted lines least-squares fits of maxima.

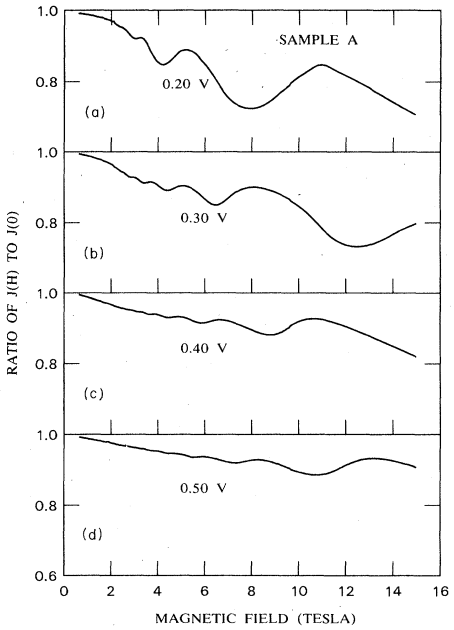

FIG. 11. Dependence of the ratio of current density at magnetic field H and constant V_G to current density at zero magnetic field at V_G on magnetic field for sample A.

Alternatively, if V_G is constant, the number of electrons in the accumulation layer is constant. Changing H sweeps successive maxima and minima of the density of states through the Fermi level. Such measurements are illustrated in Fig. 11 in which the ratio $J(H)/J(0)$ is plotted as a function of magnetic field for different values of V_G. If spin splitting is ignored, Eq. (1) can be put in the form

$$N = \frac{1}{H_z}(E_F - E_0)\frac{m}{e\hbar} - C \ , \tag{4}$$

where $C = \frac{1}{2}$ for maxima and $C = 1$ for minima.[36] Each successive maximum (minimum) in the tunnel current corresponds to the passage of a maximum (minimum) in the density of states through E_F. In Fig. 12 N is plotted as a function of the value of $10/H$ corresponding to maxima or minima. The linearity of the points is good; the maxima extrapolate to $-\frac{1}{2}$, the minima to -1. From the slope of the plots of Fig. 12, the surface concentration N_S can be obtained by using Eqs. (3) and (4), assuming that only one subband is present in the accumulation layer. Figure 13 shows N_S as a function of V_G. The solid lines are least-squares fits of data below $V_G = 0.3$ V and above $V_G = 0.3$ V. The dotted line is the extrapolation of the lower solid line. There is a clear break at $V_G \sim 0.3$ V, corresponding to $N_S \sim 7 \times 10^{11}/\text{cm}^2$. This represents the onset of the occupation of the second subband in the accumulation layer. For $V_G > 0.3$ V approximately 10% of the carriers go into a second subband. The points for $V_G \gtrsim 0.4$ V in Fig. 10, and for the Landau minima with $N = 1$ and $N = 2$, deviate from the line through the points at lower V_G. Both figures show the start of occupation of a second subband. Extrapolation of N_S to zero gives $V_T = 0.032$ V, in excellent agreement with the value ob-

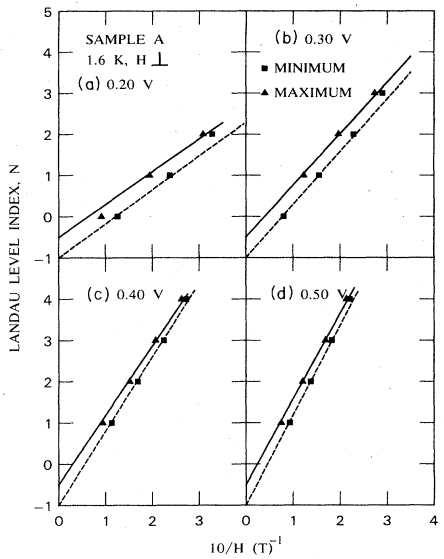

FIG. 12. Dependence of the Landau-level index N, corresponding to maxima and minima of the ratio $J(H)/J(0)$ at constant V_G on inverse magnetic field for sample A.

tained from G-V curves and from the fan diagram of Fig. 10.

For inversion layers on silicon MOS structures the surface concentration is given by $N_S = C_{ox}(V_G - V_T)$, where C_{ox} is the capacitance of the SiO_2 gate dielectric. The dashed line in Fig. 13 shows $C_I(V_G - V_T)$, where C_I is the insulator capacitance obtained by extrapolating C_I to 1.6 K in Fig. 3. N_S from this curve is higher than obtained from curves such as those of Fig. 11. However, from Fig. 7, ψ_S and ψ_G are not fixed but increase as V_G increases. Not all of the gate voltage appears across the $Al_xGa_{1-x}As$ layer. In view of the uncertainties of the ratio of V_I/V_G and of the value of C_I from a classical SIS calculation, the agreement of the solid and dashed curves of Fig. 13 is reasonable. The lower line is the surface concentration obtained by integrating the experimental 100-kHz C-V curve at $H=0$. It gives N_S a lower value than that of Fig. 11. According to Eq. (1) the splitting of a two-dimensional density of states into Landau levels is proportional to the normal component of H. We observe no Landau-level structure in tunneling curves when the magnetic field is parallel rather than perpendicular to the sample. This shows that structure is due to tunneling from Landau levels in the accumulation layer on n^--type GaAs rather than from Landau levels in bulk GaAs.

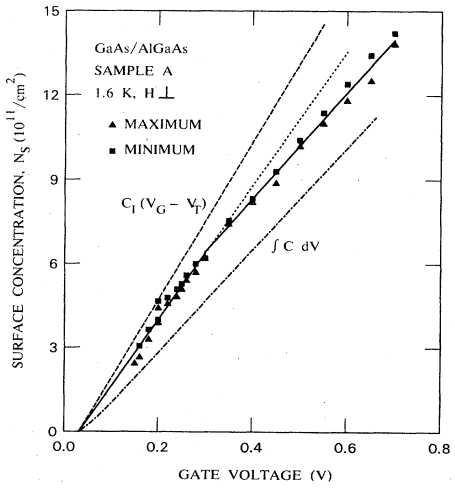

FIG. 13. Dependence of electron concentration in the accumulation layer of sample A on V_G.

Sample B

Tunneling from accumulation layers

As shown in Table I, sample B is characterized by lower charge in the $Al_xGa_{1-x}As$ layer, by a greater insulator thickness and by slightly higher doping of n^--type GaAs. Structure in tunneling from accumulation layers is more complex because of the occurrence of spin-splitting of Landau levels at high magnetic fields.

Figure 14 shows I-V curves for $V_G > 0$ V as a function of magnetic field for sample B. Current at a given voltage is lower than for sample A over most of the voltage range. The large decrease in current between 0 and 0.1 V as H increases, which is seen in Fig. 8 for sample A is not found for sample B because $V_T < 0$ V for sample B. The difference between $\log_{10}J(H)$ and $\log_{10}J(0)$ is plotted in Fig. 15. Oscillations are observed even at 2 T. At higher values of H, the structure is substantially more complex than in Fig. 9 for sample A. In order to show the development of structure as H increases, we plot C-V and $\log_{10}G$-V (G-V) curves at 100 kHz, and $\log_{10}J(H)$-$\log_{10}J(0)$ (I-V) for different magnetic fields in Figs. 16–18. Here, the ac and dc measurements complement each other. V_T for sample B is ~ -0.030 V; at 0 V an accumulation layer is already formed. dc—I-V curves are

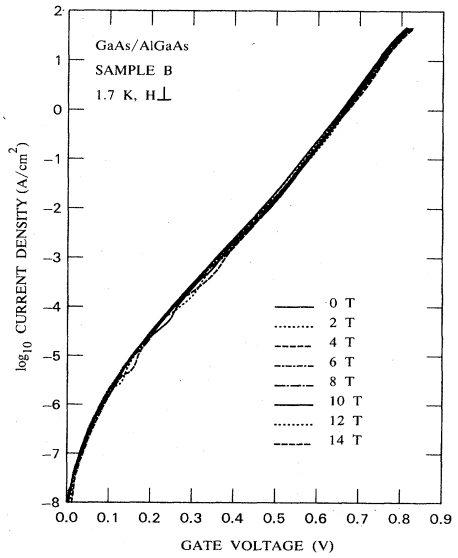

FIG. 14. $\log_{10}$ current density versus gate voltage for sample B at different magnetic fields.

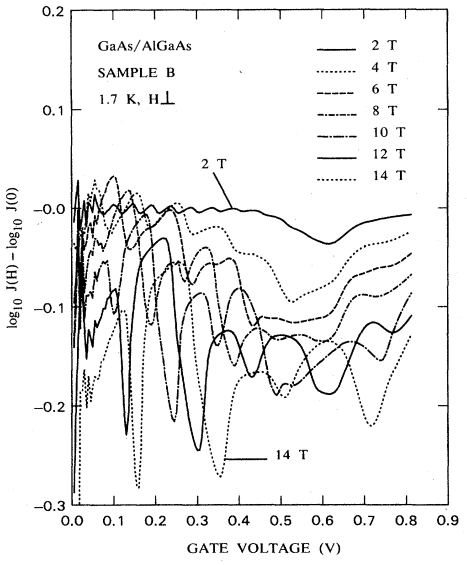

FIG. 15. Difference between $\log_{10}J$ at magnetic field H and $\log_{10}J$ at zero magnetic field as a function of gate voltage for sample B.

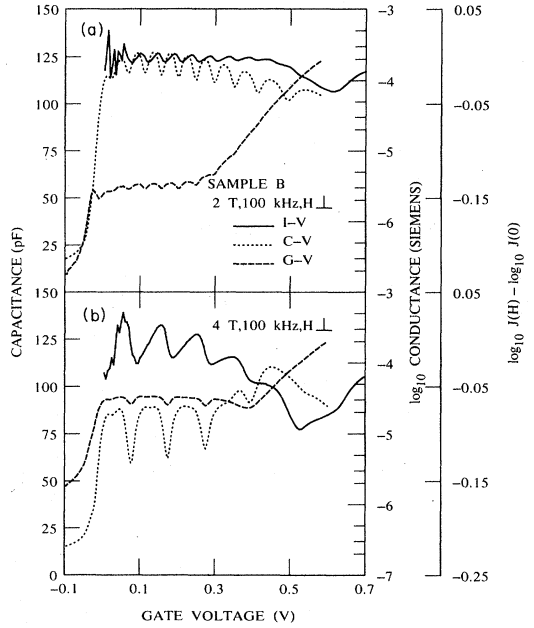

FIG. 16. Plots of $[\log_{10}J(H)-\log_{10}J(0)]$ (I-V), and of capacitance-voltage and $\log_{10}$ conductance-voltage curves at 100 kHz, versus V_G at different constant magnetic fields for sample B. (a) $H=2$ T. (b) $H=4$ T.

noisy and of uncertain reliability below $\sim$0.080 V because tunnel currents are very small. However, ac curves can be measured for $V_G < V_T$ as well as around 0 V; they show the development of the accumulation layer and of the first Landau level better than I-V characteristics. I-V characteristics can be measured to higher voltages than C-V or G-V curves and therefore show structure in higher Landau levels. I-V characteristics are also not distorted by the high-series resistance due to magnetic freezeout of the n^--type GaAs substrate. These features of the different curves are shown in Figs. 16—18.

In Fig. 16(a) structure due to many Landau levels appears in the three curves at 2 T. The spacing is constant below $V_G \sim 0.3$ V; at higher voltages the spacing broadens due to the onset of the occupation of a second subband. Tunneling from Landau levels is proportional to the number of carriers at the Fermi level. The capacitance $C=\partial Q_A/\partial V_G$, where Q_A is the charge in the accumulation layer, is proportional to the rate of change of carriers with V_G. Although the voltage spacing is constant for I-V, C-V, and G-V curves the voltage positions of extrema in C-V and G-V curves are shifted with respect to those of I-V curves. Thus the voltage for maximum rate of change of carriers is displaced with respect to tunneling curves. In Fig. 16(b), at 4 T, splitting appears in the first Landau level for C-V and G-V curves but cannot be resolved in I-V curves. At 6 T, in Fig. 17(a), spin splitting occurs in the first two Landau levels in C-V curves and in G-V curves. It is also visible in the second and third Landau levels of the I-V curves. As shown schematically in Fig. 2(b), the density of states at the center of a Landau level should be higher than the average density of states when $H=0$ T. This is reflected in the I-V curves for 2—6 T, where the maximum value of $\log_{10}J(H)-\log_{10}J(0)$ is greater than 1.0 for the lowest Landau levels. The maximum tunneling current is higher when the magnetic field is applied.

At 8 T and higher, capacitance below 0.3 V is almost completely suppressed by the high series resistance, although that structure which can be resolved corresponds to structure in G-V curves. In every case there is a steep rise in capacitance to values corresponding to those when

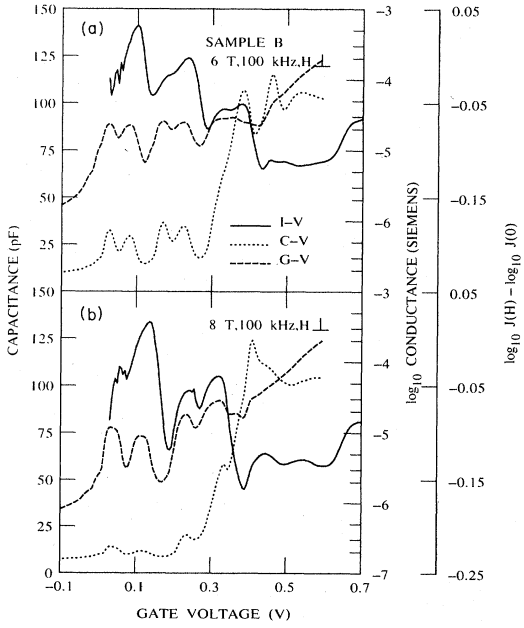

FIG. 17. Plots of $[\log_{10}J(H)-\log_{10}J(0)]$ (I-V), and of capacitance-voltage and $\log_{10}$ conductance-voltage curves at 100 kHz, versus V_G at different constant magnetic fields for sample B. (a) $H=6$ T. (b) $H=8$ T.

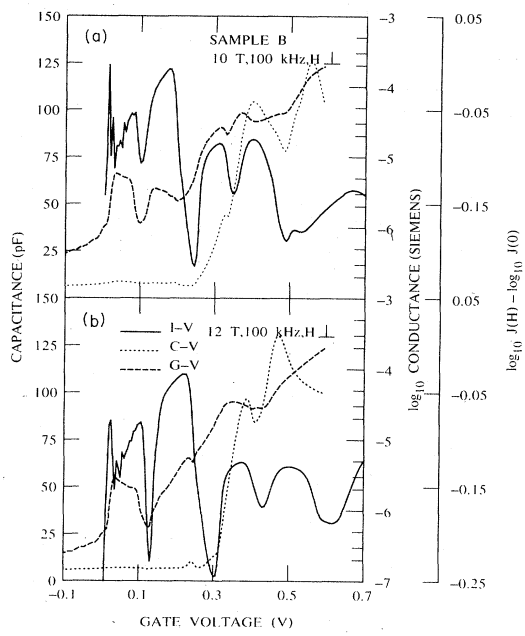

FIG. 18. Plots of $[\log_{10}J(H)-\log_{10}J(0)]$ (I-V), and of capacitance-voltage and $\log_{10}$ conductance-voltage curves at 100 kHz, versus V_G at different constant magnetic fields for sample B. (a) $H=10$ T. (b) $H=12$ T.

no field is applied at $V_G \sim 0.3$ V. This is also the gate voltage at which a second subband starts to be populated. At 12 T two Landau levels are populated and spin splitting is resolved for both in I-V curves.

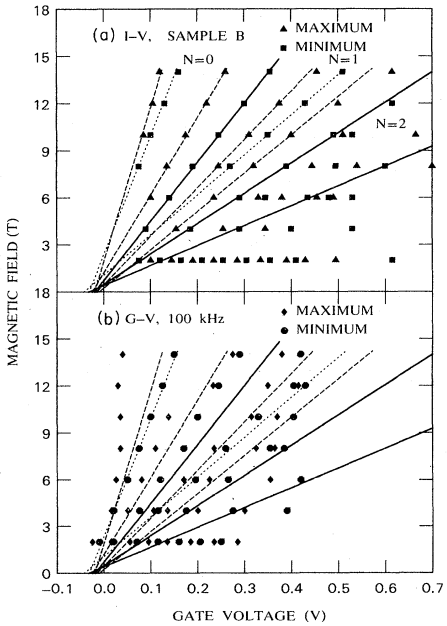

FIG. 19. (a) Fan diagram of the maxima and minima of $\log_{10}J(H)-\log J(0)$ for sample B. The solid lines are least-squares fits of minima, the dotted lines are least-squares fits of spin-split minima, and the dashed lines are fits of maxima. (b) Fan diagram of the maxima and minima of $\log_{10}G$ for sample B. The lines are the same lines as drawn for I-V curves in (a).

The fan diagram for sample B is shown in Fig. 19(a) for dc I-V curves and in Fig. 19(b) for G-V curves at 100 kHz. The best defined points on the fan diagram are the minima of I-V curves that occur on the completion of a Landau level. The solid lines in Fig. 19(a) are drawn through these points, the dotted lines are drawn through minima in spin-split Landau levels, and the dashed lines are drawn through the maxima of the spin-split Landau levels. In addition, the linearity is good for $V_G < 0.4$ V.

The value of V_T from extrapolation of the I-V fan diagram is -0.020 V. I-V curves are not distorted by the high resistance of the frozen-out n^--type GaAs, but it is not possible to determine extrema for $V_G \lesssim 0.080$ V because of the noise in measuring low tunneling currents. G-V curves as in Fig. 16—18 can show the onset of the formation of the accumulation layer but may be distorted by high-series resistance. Extrema from G-V curves are plotted in a fan diagram in Fig. 19(b). The lines are the same lines used to connect I-V points in Fig. 19(a). Just as in Fig. 10 for sample A, the first maximum of the G-V curve depends only slightly on H. The positions of other extrema are proportional to H. The minima at the completion of a Landau level are consistently at lower voltages in G-V curves than in I-V curves; the minima of spin-split Landau-level maxima, which are joined by the dotted lines, coincide. Part of the disagreement of the voltage for maxima of G-V and I-V curves at high magnetic fields is due to the width of the maxima. For example, at 10 T in Fig. 18(a), the second maximum is broad and slopes in such a way that the maximum is at a lower voltage for the G-V curve than for the I-V curve, although the width of the two maxima is nearly equal. A second reason for the disparity is that at large H, the order of magnitude rise in G overlaps the structure due to Landau levels and modifies the position of extrema.

Figure 20 shows typical plots of the ratio of $J(H)/J(0)$

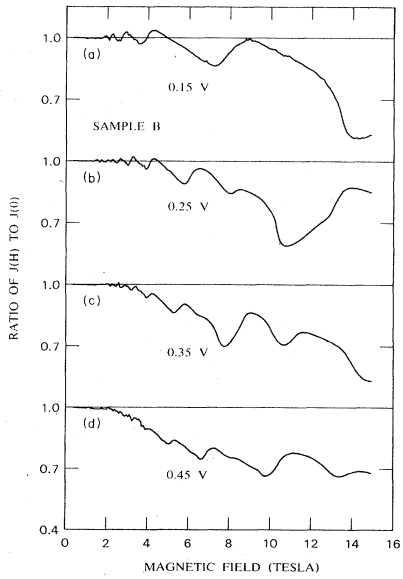

FIG. 20. Dependence of the ratio of current density at magnetic field H and constant V_G to current density at zero magnetic field at V_G on magnetic field for sample B.

at constant V_G as the magnetic field is swept, for different values of V_G. For low V_G and low H, as shown in Figs. 20(a) and 20(b), the maximum tunneling current is larger than it is with no magnetic field present. The structure at high H is more complex than in Fig. 11 because of spin splitting of Landau levels. In Fig. 21 the value of the Landau-level index, N, is plotted versus $1/H$ for the curves of Fig. 20. The better quality of sample B compared to sample A is shown by the observation of more Landau levels in Fig. 21 as compared to Fig. 12. In Fig. 21, minima corresponding to high values of N fall on the minimum line that extrapolates to -1. As H increases and N decreases the Landau levels are spin split and the center of the Landau level changes from a maximum to a minimum, as shown schematically in Fig. 2(c). This is reflected in the plots of minima in Fig. 21; at low values of $1/H$ the minima shift to the line through the maxima corresponding to higher values of N. Surface concentrations as a function of V_G for sample B are shown in Fig. 22. Tunneling current at constant V_G was measured at 0.050-V increments for H increasing and at 0.020-V increments for H decreasing to determine N_S. The solid line in Fig. 22 is drawn through points derived from tunneling curves for increasing H. The points for decreasing H give slightly higher values of N_S at a given V_G. The discrepancy is probably due to trapped flux in the superconducting magnet which affects the value of H used in plots such as those of Fig. 20. The effect is more pronounced in sample B than in sample A, since N_S is derived from Landau levels with higher values of N that occur at lower values of H. Trapped flux is more important at low H than at high H. There is evidence for occupation of a second subband at $N_S \sim 8\times10^{11}/\text{cm}^2$. At $V_G = 0.65$ V the marked decrease in N_S, which is derived

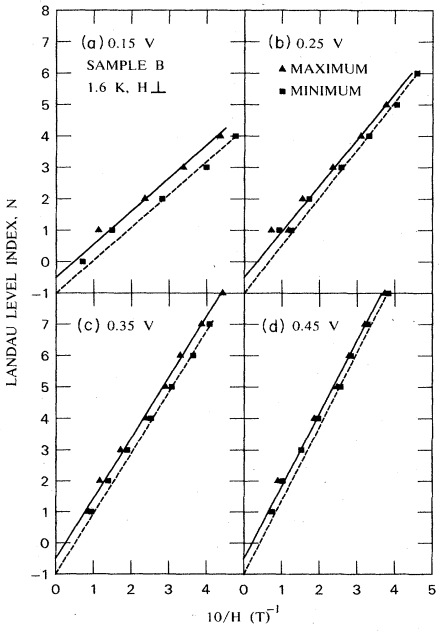

FIG. 21. Dependence of the Landau-level index N, corresponding to maxima and minima of the ratio $J(H)/J(0)$ at constant V_G on inverse magnetic field for sample B.

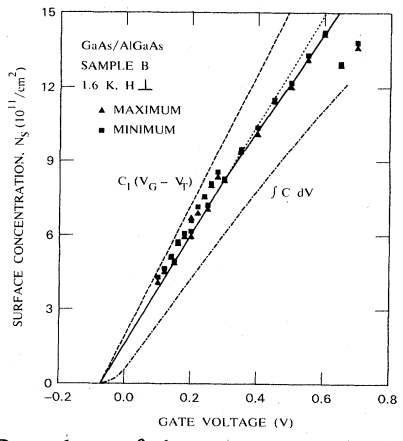

FIG. 22. Dependence of electron concentration in the accumulation layer of sample B on V_G.

by assuming a single Landau level is occupied, indicates that a significantly larger fraction of the carriers are going into the second subband. As in Fig. 13, N_S calculated from C_I derived from C-V curves above 100 K is higher than N_S measured by tunneling curves while N_S obtained by integrating C-V curves is lower. Ando[37] and Stern and DasSarma[38] have calculated that occupation of the second subband of an accumulation layer should begin at $N_S \sim 3\times10^{11}/\text{cm}^2$ which is less than half the value we find, but the calculated value depends on minority carrier concentration and other sample parameters that are not well known.

Tunneling from n^+-type GaAs into n^--type GaAs

When $V_G < 0$ V, electrons tunnel from n^+-type GaAs into n^--type GaAs. For sample A, I-V curves at high H are modulated with a voltage period, 0.0360 V, which is slightly less than the optical value of the LO phonon energy in GaAs, 0.0367 eV.[27,39] However, such periodicities are not seen for sample B. Figure 23 shows the I-V curves for sample B for $V_G < 0$ V and for different mag-

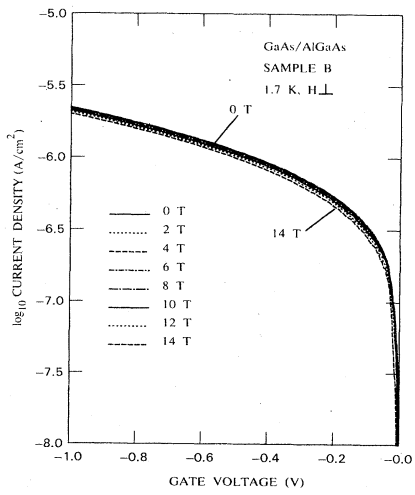

FIG. 23. $\log_{10}$ of current density versus gate voltage for sample B biased into depletion for different magnetic fields.

netic fields, and Fig. 24 shows $d\ln(J)/dV_G$ for the I-V curves at different values of H. The ordinate is the same for all the curves of Fig. 24, but the curves are displaced for clarity. The thickness of sample B, derived from C-V curves and given in Table I, is 22.0 nm which is ~ 1.5 nm greater than that of sample A. As a result the current densities are almost 2 orders of magnitude smaller for sample B. As shown in Fig. 24, there is periodic modulation of the derivative curve at 0 and 2 T. However the period is 0.030 V, not 0.036 V as for sample A. At higher H this periodicity is suppressed, in contrast to sample A in which phonon periodicities are enhanced at high H. It is not certain whether the periodicity at 0 T is real or not; the currents are so low that it may be an artifact of the measurement. It is also not known why 0.036-V periodicities are not observed but the most probable reason is the low value of tunnel current due to the thicker barrier. Recently Eaves and co-workers[40,41] have observed modulation of I-V curves in reverse bias of an AlGaAs capacitor. The period was 0.036 V, but no magnetic field was required to observe the modulation and periodicities were observed in I-V characteristics up to 50 K. It is clear that much more systematic work is required to elucidate the mechanism or mechanisms responsible for modulation of I-V curves for direct tunneling through $Al_xGa_{1-x}As$ barriers.

DISCUSSION

The results presented here are the initial measurements of the effect of magnetic field on direct tunneling from accumulation layers in AlGaAs capacitors. They are on a limited set of samples; no systematic investigation has been made of parameters that affect tunneling through $Al_xGa_{1-x}As$. Even so, they show a richness of phenomena that demonstrates the near ideality of the system for studying tunneling in semiconductors.

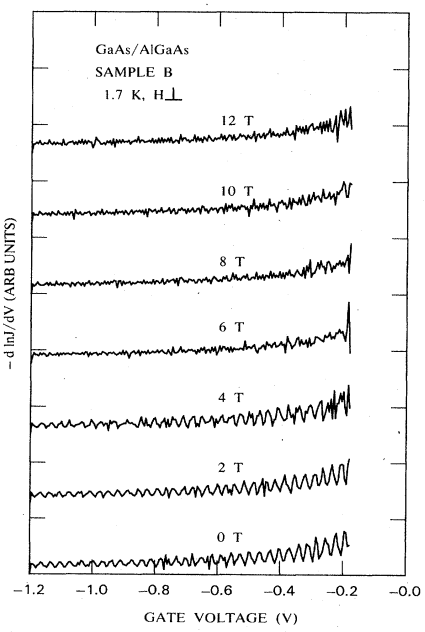

FIG. 24. Derivative of natural logarithm of current density versus V_G for sample B for different magnetic fields. The curves have been offset vertically for clarity but are all on the same scale.

The dependence of the density of states in a two-dimensional inversion or accumulation layer on magnetic field is an important factor in determining many physical properties of the system. Shubnikov—de Haas (SdH) measurements of transport parallel to the surface in a 2DEG have been the most commonly used method of showing the presence of a 2DEG as well as studying its properties.[1] SdH measurements involve both the density of states in a 2DEG and the mobility of carriers parallel to the surface. Observations of the quantum Hall effect and fractional quantum Hall effect show the existence of extended states at the center of a Landau level and of localized states between Landau levels.[42] Magnetocapacitance measurements of modulation-doped heterostructures have been used to derive the density of states in the 2DEG.[26] de Haas—van Alphen (dHvA) measurements[43,44] and specific-heat measurements[45] of multiple GaAs/$Al_xGa_{1-x}As$ heterostructures have recently been used to determine equilibrium densities of states in a 2DEG on GaAs. The two-terminal I-V and C-V measurements reported here show that tunneling depends on the density of states in Landau levels in the accumulation layer. Although they are transport measurements they differ from conventional SdH measurements in that carrier transport in the 2DEG parallel to the surface is not required. Even when electrons in GaAs are frozen out by the high magnetic fields, there should be a large supply of electrons available to the accumulation layer from the n^+ substrate. The density of states for tunneling is a single-particle density of states that also differs from the equilibrium density of states measured by dHvA or specific-heat measurements. With the development of suitable tunneling models it may eventually be possible to extract the density of states from tunneling measurements.

Comparison of results for samples A and B shows that the accumulation layer differs for the two samples. Experimentally, the strongest differences are the observation of Landau-level structure at 2 T and the observation of spin splitting in all Landau levels for sample B. As shown in Table I, one difference between the two samples is the amount of negative charge in the $Al_xGa_{1-x}As$ layer N_I, where sample A has over twice as much as sample B. Such negative charge can scatter carriers in the accumulation layer and reduce their lifetime. A second difference between the two samples may be the homogeneity of the samples. This cannot be quantified by measurements on two-terminal structures such as AlGaAs capacitors, but may eventually be characterized by measurements of GaAs—gate-field-effect transistors in which carrier mobilities parallel to the surface can be determined.[46]

The excellent resolution of peaks due to spin splitting in sample B is surprising. The g factor for bulk GaAs, ~ 0.5, is small.[47] Enhancement of the g factor by electron-electron exchange effects has been observed by SdH measurements on modulation-doped GaAs/$Al_xGa_{1-x}As$ heterostructures.[48–51] Values up to $g \sim 5$ have been suggested. A value of $g=0.19$ has been report-

ed from cyclotron resonance measurements.[52] We are unable to give a value of g. Changing V_G for an AlGaAs capacitor changes N_S by an amount proportional to V_G, but this does not mean that ΔE_F is linearly proportional to ΔV_G.[53] To determine g, it is necessary to have a degeneracy between spin-split levels of different Landau-level index by tilting the magnetic field with respect to the sample.[54] The GaAs system is an unfavorable one to do this because of the small effect mass of electrons.

ACKNOWLEDGMENTS

This work would not have been possible without the superconducting magnet which was made available through the courtesy of F. F. Fang, or the samples provided by H. Morkoç. M. Thomas assisted greatly with the measurements. Conversations with F. Stern, F. F. Fang, and P. M. Solomon are much appreciated.

[1]For a review, see T. Ando, A. B. Fowler, and F. Stern, Rev. Mod. Phys. **54**, 437 (1982).
[2]D. J. BenDaniel and C. B. Duke, Phys. Rev. **160**, 679 (1967).
[3]D. C. Tsui, Phys. Rev. Lett. **24**, 303 (1970).
[4]D. C. Tsui, Solid State Commun. **8**, 113 (1970).
[5]D. C. Tsui, Solid State Commun. **9**, 1789 (1971).
[6]D. C. Tsui, Phys. Rev. B **4**, 4438 (1971).
[7]D. C. Tsui, in *Proceedings of the 10th International Conference of Physics of Semiconductors, Cambridge, 1970,* edited by S. Keller, J. C. Hensel, and F. Stern (U.S. AEC, Oak Ridge, 1970), p. 468.
[8]D. C. Tsui, Phys. Rev. B **8**, 2657 (1973).
[9]D. C. Tsui, Phys. Rev. B **12**, 5739 (1975).
[10]J. A. Appelbaum and G. A. Baraff, Phys. Rev. B **4**, 1246 (1971).
[11]G. A. Baraff and J. A. Appelbaum, Phys. Rev. B **5**, 475 (1972).
[12]D. S. Tsui, G. Kaminsky, and P. H. Schmidt, Phys. Rev. B **9**, 3524 (1974).
[13]W. Thoren, G. Heiland, D. Kohl, H. von Lohneysen, W. Platen, and H. J. Schink, Surf. Sci. **137**, 293 (1984).
[14]U. Kunze and G. Lautz, Solid State Commun. **42**, 27 (1982).
[15]U. Kunze, J. Phys. C **17**, 5677 (1984).
[16]E. Kress-Rogers, G. F. Hopper, R. J. Nicholas, W. Hayes, J. C. Portal, and A. Chevy, J. Phys. C **16**, 4285 (1984).
[17]T. Hagiwara, O. Mizuno, and S. Tanaki, J. Phys. Soc. Jpn. **34**, 973 (1973).
[18]V. A. Berezovets, I. I. Farbshtein, and S. L. Shelankov, Fiz. Tverd. Tela (Leningrad) **25**, 2988 (1983) [Sov. Phys.—Solid State **25**, 1725 (1983)].
[19]W. A. Berk and J. R. Anderson, Bull. Am. Phys. Soc. **30**, 383 (1985).
[20]P. M. Solomon, T. W. Hickmott, H. Morkoç, and R. Fischer, Appl. Phys. Lett. **42**, 821 (1983).
[21]T. W. Hickmott, P. M. Solomon, R. Fischer, and H. Morkoç, J. Appl. Phys. **57**, 2844 (1985).
[22]T. W. Hickmott, P. M. Solomon, R. Fischer, and H. Morkoç, Appl. Phys. Lett. **44**, 90 (1984).
[23]For a review of tunneling in semiconductors, see D. C. Tsui, in *Handbook on Semiconductors,* edited by T. S. Moss and W. Paul (North-Holland, Amsterdam, 1982), Vol. 1, p. 661.
[24]A. G. Chynoweth, R. A. Logan, and P. A. Wolff, Phys. Rev. Lett. **5**, 548 (1960).
[25]A. M. Voshchenkov and J. Zemel, Phys. Rev. B **9**, 4410 (1974).
[26]T. P. Smith, B. B. Goldberg, P. J. Stiles, and M. Heiblum, Phys. Rev. B **32**, 2696 (1985).
[27]T. W. Hickmott, P. M. Solomon, F. F. Fang, F. Stern, R. Fischer, and H. Morkoç, Phys. Rev. Lett. **52**, 2053 (1984).
[28]T. W. Hickmott, P. M. Solomon, F. F. Fang, R. Fischer, and H. Morkoç, in *Proceedings of the 17th International Conference on Physics of Semiconductors, San Francisco, 1984,* edited by J. D. Chadi and W. A. Harrison (Springer, New York, 1985), p. 417.
[29]D. Shoenberg, J. Low Temp. Phys. **56**, 417 (1984).
[30]Samples were grown by H. Morkoç, University of Illinois.
[31]Y. Yafet, R. W. Keyes, and E. N. Adams, J. Phys. Chem. Solids **1**, 137 (1956).
[32]F. F. Fang has observed the effect of Landau levels on capacitance-voltage curves of AlGaAs capacitors (unpublished).
[33]E. H. Nicollian and J. R. Brews, *MOS Physics and Technology* (Wiley, New York, 1982), p. 385.
[34]T. O. Poehler, Phys. Rev. B **4**, 1223 (1971).
[35]H. U. Baranger and J. W. Wilkins, Phys. Rev. B **30**, 7349 (1984).
[36]E. J. Pakulis, Phys. Rev. B **31**, 6807 (1985).
[37]T. Ando, J. Phys. Soc. Jpn. **51**, 3893 (1982).
[38]F. Stern and S. DasSarma, Phys. Rev. B **30**, 840 (1984).
[39]J. S. Blakemore, J. Appl. Phys. **53**, R123 (1982).
[40]L. Eaves, P. S. S. Guimaraes, B. R. Snell, D. C. Taylor, and K. E. Singer, Phys. Rev. Lett. **55**, 262 (1985).
[41]P. S. S. Guimaraes, D. C. Taylor, B. R. Snell, L. Eaves, K. E. Singer, G. Hill, M. A. Pate, G. A. Toombs, and F. W. Sheard, J. Phys. C **18**, 1605 (1985).
[42]H. L. Störmer and D. C. Tsui, Science **220**, 1241 (1983).
[43]H. L. Störmer, T. Haavasoja, V. Narayanamurti, A. C. Gossard, and W. Wiegmann, J. Vac. Sci. Technol. B **1**, 423 (1983).
[44]J. P. Eisenstein, H. L. Störmer, V. Narayanamurti, and A. C. Gossard, Superlattices Microstruct. **1**, 11 (1985).
[45]E. Gornik, R. Lassnig, G. Strasser, H. L. Störmer, A. C. Gossard, and W. Wiegmann, Phys. Rev. Lett. **54**, 1820 (1985).
[46]P. M. Solomon, C. M. Knoedler, and S. L. Wright, IEEE Trans. Electron. Dev. **ED-5**, 379 (1984).
[47]C. Weisbuch and C. Hermann, Phys. Rev. B **15**, 816 (1977).
[48]S. Narita, S. Takeyama, W. B. Luo, S. Hiyamizu, K. Nanbu, and H. Hashimoto, Jpn. J. Appl. Phys. **20**, L437 (1981); L861 (1981).
[49]R. J. Nicholas, M. A. Brummell, and J. C. Portal, Surf. Sci. **113**, 290 (1982).
[50]T. Englert, D. C. Tsui, A. C. Gossard, and C. Uihlein, Surf. Sci. **113**, 295 (1982).
[51]S. Narita, S. Takeyama, W. B. Luo, S. Hiyamizu, K. Nanbu, and H. Hashimoto, Surf. Sci. **113**, 301 (1982).
[52]D. Stein, K. v. Klitzing, and G. Weimann, Phys. Rev. Lett. **51**, 130 (1983).
[53]H. L. Störmer, Jpn. J. Appl. Phys. **20**, 1859 (1981).
[54]F. F. Fang and P. J. Stiles, Phys. Rev. **174**, 823 (1968).